Int. J. Morphol.,
44(2):660-668, 2026.

Three-Dimensional Evaluation of the Morphometry and Spatial Relationship of the Superior Orbital Fissure and Optic Canal

Evaluación Tridimensional de la Morfometría y la Relación Espacial de la Fisura Orbitaria Superior y el Canal Óptico

Fatma Yasemin Öksüzler[1]; Mahmut Tunç[2]; Sema Polat[3]; Esin Özsahin[4]; Zafer Altun[5] & Pınar Göker[3]

ÖKSÜZLER, F. Y.; TUNÇ, M.; POLAT, S.: ÖZSAHIN, E.; ALTUN, Z. & GÖKER, P. Three-dimensional evaluation of the morphometry and spatial relationship of the superior orbital fissure and optic canal. *Int. J. Morphol., 44(2)*:660-668, 2026.

SUMMARY: This study aims to evaluate the morphology and morphometry of the superior orbital fissure (SOF) and optic canal (OC), and to analyze their spatial relationship with one another. This retrospective study included dento-maxillofacial CT images from 132 healthy individuals (71 females and 61 males), with a mean age of 35.33±11.48 years. The images were imported into 3D Slicer (version 5.6.2). Measurements of the SOF included its minimum and maximum widths, lengths, and areas. For the OC, vertical and horizontal diameters, as well as the area, were evaluated. Additionally, the distances from the OC to the lateral, middle, and medial points of the SOF were recorded. The morphological classification of the SOF was also conducted, categorizing its shape into seven distinct types. Age-based subgroup analysis showed significant differences in both the vertical diameter of the optic canal ($p=0.039$) and the minimum width of the superior orbital fissure ($p=0.019$) across different age decades. The morphological classification of the SOF identified the keyhole-shaped type (Type 5) as the most prevalent form (19.7 %), while the straight type (Type 2) was the least frequently observed (9.8 %). Statistically significant differences were found in all SOF-related morphometric parameters among the different morphological types ($p<0.05$), except for the distance between the optic canal and the lateral margin of the SOF. Comprehensive knowledge of normative morphometric parameters is crucial not only for accurate surgical planning and precise delineation of operative boundaries but also for substantially minimizing the risk of intraoperative complications.

KEY WORDS: Superior orbital fissure: Orbital apex; Optic canal; Morphometry; Morphology.

INTRODUCTION

The bony orbit is best described as a pyramid with either a conical or quadrangular base. The anterior segment of the pyramid comprises the orbital rim, which forms the base; whilst the posterior segment is constituted by the orbital apex (Abed *et al*., 2011). The orbital apex is defined as the area between the orbit and the intracranial space. It is a site of anatomical significance, as it contains structures such as the optic canal (OC), superior orbital fissure (SOF) and inferior orbital fissure (IOF). Collectively, these structures form an opening to the orbit (Engin *et al*., 2021). The contents of the superior orbital fissure and the optic foramen are the structures that are most likely to be affected by pathology at the apex of the orbit (Abed *et al*., 2011). The superior orbital fissure (SOF) is a diminutive topographically significant area that connects the middle cranial fossa and the orbit. This critical three-dimensional area is distinguished by its highly variable shape and is located lateral to and below the optic canal at the apex of the orbit. It is bounded medially by the lesser wing of the sphenoid, inferiorly and laterally by the greater wing of the sphenoid, and superiorly by the frontal bone (Reymond *et al*., 2008; La Marra *et al*., 2016). The SOF is topographically divided into two parts; The superior or superolateral part contains the trochlear, lacrimal, frontal nerves and superior ophthalmic vein, while the inferior or inferomedial part contains the superior and inferior branches of the oculomotor nerve, the nasociliary nerve, the abducens nerve, the sensory root of the ciliary ganglion and the sympathetic root. The inferior ophthalmic vein, if present in this location, may on occasion traverse the tendinous annulus of Zinn (La Marra *et al*., 2016).

[1] Izmir Democracy University Buca Seyfi Demirsoy Training And Research Hospital, Department of Radiology, Izmir, Turkey.
[2] Baskent University, Vocational School of Health Services, Department of Therapy and Rehabilitation, Adana, Turkey.
[3] Cukurova University Faculty of Medicine, Department of Anatomy, Adana, Turkey.
[4] Baskent University Faculty of Medicine, Department of Anatomy, Adana, Turkey.
[5] Baskent University, Adana Dr. Turgut Noyan Application and Research Center, Department of Radiology, Adana, Turkey.

Received: 2025-11-22 Accepted: 2026-02-06

The optic canal represents another significant anatomical structure in the orbital apex region. The optic canal (OC) is located at the superior aspect of the orbit, forming a connection between the orbit and the middle cranial fossa. The optic nerve, ophthalmic artery, dura mater, arachnoidea mater and sympathetic fibres all pass through this structure. The OC is comprised of three constituent parts: the orbital aperture, the intermediate section (referred to as the "optic waist"), and the intracranial aperture (Reymond *et al*., 2008; Pirinc *et al*., 2023). The surgical approach to the site of interest has been demonstrated to increase the risk of iatrogenic injury to neural and vascular structures (Sinanoglu *et al*., 2016). The proximity of the bone to nerve fibres in the OC has been identified as a locus minoris resistentiae in the event of injury or any expansive processes affecting the optic nerve (ON). Decompression of the ON is one of the most frequently performed neurosurgical procedures in the OC. A comprehensive understanding of the anatomical structure of the OC and the ON is paramount for the effective diagnosis and treatment of diseases affecting the ON, the brain, the paranasal sinuses, and the bones of the skull. The use of modern radiological techniques such as magnetic resonance imaging and computed tomography forms the basis of the preoperative diagnostic approach to the OC and ON, while research methods based on anatomy (i.e. morphometry) have the potential to generate novel concepts for surgical intervention in the OC and ON (Radunovic *et al*., 2019).

The anatomical position of the optic canal, optic nerve and SOF is significant for surgical approaches. Furthermore, the anatomical position of the optic nerve is of paramount importance for any procedure that requires access to the SOF and the intraconal space. For example, when accessing the optic nerve through endoscopic endonasal approaches, it is important to ensure that the SOF is located lateral to the optic nerve. This ensures that as long as the SOF is not exceeded, the optic nerve is protected (Li *et al*., 2020; Erbek *et al*., 2024). This study has two primary objectives: to characterize the morphometry and morphology of the superior orbital fissure and optic canal, and to highlight the clinical significance of their spatial relationship. The results aim to offer valuable insights for researchers, surgeons, and clinicians involved in related disciplines.

MATERIAL AND METHOD

Subjects

This retrospective study included dento-maxillofacial CT images from 132 individuals (71 females and 61 males) with a mean age of 35.33±11.48 years. The inclusion criteria were as follows: age between 18 and 65 years; absence of systemic diseases affecting measurements; no history of surgery, deformity, or pathology (such as tumors or fractures) in the relevant region; no existing ocular diseases; and high-quality images free from artifacts. Based on power analysis, the minimum required sample size was determined to be 96 radiographic units at a 95 % confidence level, with a = 0.05, d = 0.10, and p = 0.50. Additionally, for sex-based comparisons, a total sample size of 128 (64 individuals per sex group) was calculated to achieve 80 % power with an effect size of 0.5 at the 95 % confidence level. Measurements were analyzed according to sex as well as age groups, categorized by decades: decade 1 (10–19 years), decade 2 (20–29 years), decade 3 (30–39 years), decade 4 (40–49 years), and decade 5 (50 years and above).

Study design

This study which was a retrospective observational study was approved by Clinical Researches Ethics Committee. CT examination were performed on a 16 detector multisection CT (Emotion16 Siemens, Erlangen, Germany). The images obtained in DICOM format were uploaded to 3D-Slicer (version 5.6.2), an open source software platform, and three-dimensional (3D) images were obtained by multiplanar reconstruction. In the obtained 3D images, the measurement area was revealed with appropriate cutting and clear measurements were taken. The decision on the appropriateness of the CT images to be included in this study was made by an experienced radiologist and an anatomist. All measurements were taken by an expert radiologist [Z.A.] and an anatomist [S.P.]. In order to minimise intra-observer variability, all measurements were performed randomly by consensus in different sessions at least three weeks apart from the initial assessments. The mean of the two measurements was used for the final value of all measured regions. The intraclass correlation coefficient (ICC) for the two evaluators was 0.820.

Measurements

The measurements were based on the study of Reymond *et al*. (2008) and Erbek *et al*. (2024). The measurements taken are shown in Table I. The table includes the description and abbreviations of the measurements. The measurements are also shown schematically in Figure 1. In order to take detailed measurements while measuring the width of SOF, unlike other studies, SOF was divided into two parts as upper and lower, and the narrowest part of the upper part and the widest part of the lower part were taken separately as width. In addition, the area measurements of SOF and OC were taken from the maximum image seen after the cutting and standardisation process in the 3D image. While other studies took the measurements in the anatomical

position, in the present study, the image was standardised by taking the image anteriorly for measurement. In addition, SOF morphology was evaluated according to the classification of Pirinc *et al*. (2023). According to this, SOF shape is divided into 7 different types. These are; Curved type (type 1), Straight type (type 2), Racket-shaped type (type 3), Eight shaped type (type 4), Key-shaped type (type 5), Narrow type (type 6) and Triangular type (type 7). SOF types are shown in Figure 2.

Statistical Analysis

The SPSS program was used to carry out the statistical analysis of this study. Descriptive statistics, including means, standard deviations, minimum and maximum values, were recorded. Pearson's correlation test was used for comparisons. $p<0.05$ was considered statistically significant.

Table I. Definitions and abbreviations of the measurements.

Abbrevation	Definition
SOF-Length	Maximum vertical length of the superior orbital fissure
SOF-Width-Min	Minimum horizontal width of the superior orbital fissure
SOF-Width-Max	Maximum horizontal width of the superior orbital fissure
OC-Lateralpole-SOF	Distance from the optic nerve centre to the lateral pole of the superior orbital fissure
OC-Medialpole-SOF	Distance from the optic nerve centre to the medial pole of superior orbital fissure
OC-Midpoint-SOF	Distance from the optic nerve centre to the point determined by the narrowing of the fissure
OC-Vertical	Maximum vertical length of the canalis opticus
OC-Horizontal	Maximum horizontal width of the canalis opticus
OC-Area (mm^2)	Surface area on the anterior side of the canalis opticus
SOF-Area (mm^2)	Surface area on the anterior side of the superior orbital fissure

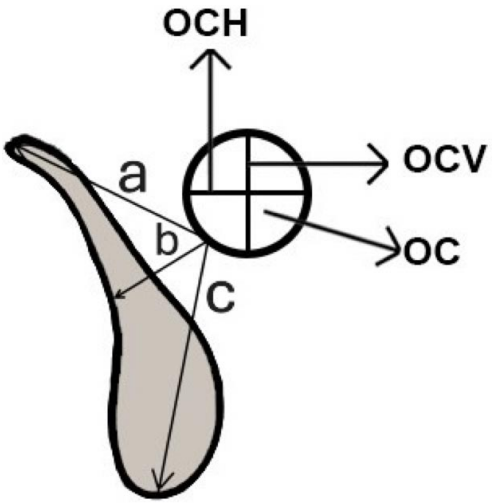

Fig. 1. Schematic drawing of superior orbital fissure and optic canal measurements. (a) distance from the optic nerve centre to the lateral pole of the superior orbital fissure, (b) distance from the optic nerve centre to the point determined by the narrowing of the fissure, (c) distance from the optic nerve centre to the medial pole of superior orbital fissure. OC: optic canal, OCV: optic canal vertical diameter, OCH: optic canal horizontal diameter.

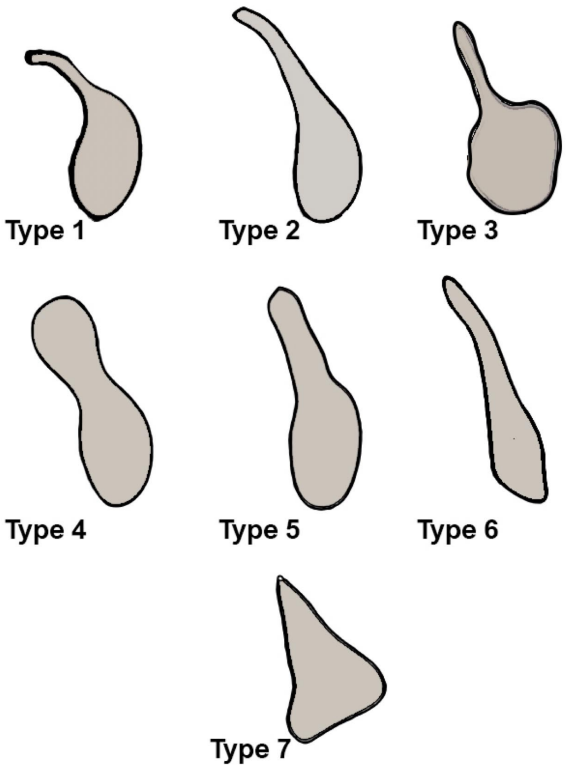

Fig. 2. Schematic representation of the shapes of the superior orbital fissure. Curved type (type 1), Straight type (type 2), Racket-shaped type (type 3), Eight shaped type (type 4), Key-shaped type (type 5), Narrow type (type 6) and Triangular type (type 7).

RESULTS

The mean age of the 132 subjects (71 females and 61 males) was 35.33±11.48 years. The mean, minimum, and maximum values of the SOF and OC measurements are presented in Table II. Sex comparison revealed a statistically significant difference only in the vertical length of the optic canal (p=0.016), while no significant differences were found in other measurements (Table III). Similarly, age-decade analysis showed statistically significant differences in the vertical length of the optic canal (p=0.039) and the minimum width of the SOF (p=0.019), whereas other measurements did not differ significantly across age groups (Table IV). Additionally, the morphological classification of the SOF was evaluated. The keyhole-shaped type (Type 5) was the most prevalent, accounting for 19.7 %, while the straight type (Type 2) was the least common at 9.8 % (Table V). When measurements were compared according to SOF types, statistically significant differences were observed in all SOF-related parameters (p<0.05), except for the distance between the optic canal and the lateral margin of the SOF (Table VI). Finally, correlation analysis was performed to assess relationships between the measurements. A weak but statistically significant correlation was found between SOF type and SOF minimum width (r=0.260; p=0.003), excluding measurements that are naturally related. Furthermore, a weak statistically significant correlation was observed between the SOF surface area and the OC surface area (r=0.386; p<0.001) (Table VII).

Table II. Mean, minimum and maximum values of the measurements.

Measurements	Mean±S.D.	Min	Max
SOF-Length	19.10±3.97	8.55	28.41
SOF-Width-Min	3.10±1.47	0.57	8.88
SOF-Width-Max	7.70±1.87	3.03	12.44
OC-Lateralpole-SOF	15.43±3.99	5.77	22.26
OC-Medialpole-SOF	7.71±1.49	4.92	13.08
OC-Midpoint-SOF	8.52±1.75	5.28	13.78
OC-Vertical	4.01±1.15	1.49	7.75
OC-Horizontal	3.71±0.82	1.81	6.64
OC-Area (mm^2)	12.77±5.16	2.90	33.00
SOF-Area (mm^2)	89.68±33.99	25.27	240.10

Table III. Distribution of measurements according to sex.

Measurements	Sex	N	Mean±S.D.	Min	Max	P value
SOF-Length	Female	71	19.05±4.11	8.83	26.13	0.870
	Male	61	19.16±3.83	8.55	28.41	
SOF-Width-Min	Female	71	3.12±1.39	1.24	8.88	0.857
	Male	61	3.07±1.56	0.57	8.66	
SOF-Width-Max	Female	71	7.79±1.98	4.03	12.44	0.562
	Male	61	7.60±1.75	3.03	12.38	
OC-Lateralpole-SOF	Female	71	15.09±4.11	5.77	21.06	0.287
	Male	61	15.83±3.84	6.01	22.26	
OC-Medialpole-SOF	Female	71	7.86±1.59	5.17	13.08	0.221
	Male	61	7.54±1.36	4.92	10.99	
OC-Midpoint-SOF	Female	71	8.42±1.70	5.33	13.21	0.496
	Male	61	8.63±1.82	5.28	13.78	
OC-Vertical	Female	71	4.24±1.18	1.91	7.75	**0.016**
	Male	61	3.75±1.07	1.49	6.87	
OC-Horizontal	Female	71	3.72±0.84	2.01	6.64	0.838
	Male	61	3.69±0.81	1.81	6.56	
OC-Area (mm^2)	Female	71	13.3±5.4	2.9	33.0	0.163
	Male	61	12.1±4.8	2.9	24.8	
SOF-Area (mm^2)	Female	71	89.5±36.5	34.7	240.1	0.952
	Male	61	89.9±31.1	25.3	167.0	

DISCUSSION

In the present study, the morphometry and morphology of the superior orbital fissure, the morphometry of the optic canal and the morphometric relationship between the superior orbital fissure and the optic canal were evaluated. In our study, OC-vertical length showed a statistically significant difference between sexes and between age deciles (p=0.016; p=0.039). In addition, SOF-Width-Minimum value was wider in early youth, narrowed in adulthood and widened again with increasing age. Furthermore, SOF was divided into 7 types in order to evaluate SOF morphologically. The present study revealed that there was no statistical difference between the SOF types. Type 5 (19.7 %) was the most frequently observed type, while Type 2 (9.8 %) was the least frequently observed. While there are statistically significant differences between the types, which are natural due to the measurements, the statistically significant difference between the types in OC-Midpoint-SOF and OC-Lateralpole-SOF measurements is noteworthy. Moreover, the results of the correlation test indicate a statistically significant yet weak relationship between SOF type and SOF-Width-Minimum width, as well as between OC-LateralPole-SOF length. It can be hypothesised that the minimum width is a factor in determining the SOF type.

The morphometric characteristics of the orbital apex hold significant importance in both orbital and maxillofacial surgical procedures. In their seminal study, Eo *et al.* (2005) investigated the effects of orbital and facial fractures on the orbital apex,

Table IV. Distribution of measurements according to age decades.

Measurements	Decade	N	Mean	SD	Min	Max	P value
	1.00	14	19.315	2.99	11.890	25.11	
	2.00	31	18.079	3.99	8.550	24.26	
SOF-Length	3.00	40	19.943	3.58	10.950	25.01	0.304
	4.00	30	19.422	4.19	8.850	28.41	
	5.00	17	18.253	4.91	8.826	24.75	
	1.00	14	3.46	1.55	1.24	6.22	
	2.00	31	2.45	1.23	0.73	6.26	
SOF-Width-Min	3.00	40	3.01	1.20	0.57	5.63	**0.019**
	4.00	30	3.35	1.61	1.46	8.66	
	5.00	17	3.76	1.76	1.36	8.88	
	1.00	14	7.99	1.77	5.84	12.44	
	2.00	31	7.21	1.81	3.03	10.23	
SOF-Width_max	3.00	40	7.71	2.01	4.27	12.38	0.442
	4.00	30	7.81	1.72	4.21	11.02	
	5.00	17	8.19	2.01	4.03	12.41	
	1.00	14	15.78	3.48	8.47	21.25	
	2.00	31	14.51	4.04	6.01	21.70	
OC-Lateralpole-SOF	3.00	40	16.11	3.69	6.37	22.26	0.398
	4.00	30	15.84	3.80	6.96	19.96	
	5.00	17	14.53	5.15	5.77	22.04	
	1.00	14	7.54	1.59	5.17	10.17	
	2.00	31	7.45	1.59	4.92	12.22	
OC-Medialpole-SOF	3.00	40	7.95	1.20	5.47	10.47	0.546
	4.00	30	7.57	1.69	5.33	13.08	
	5.00	17	7.99	1.52	5.32	10.99	
	1.00	14	8.19	1.44	6.23	11.05	
	2.00	31	8.22	1.93	5.28	13.78	
OC-Midpoint-SOF	3.00	40	8.48	1.85	5.41	13.65	0.441
	4.00	30	8.68	1.48	6.19	11.96	
	5.00	17	9.14	1.83	6.09	13.21	
	1.00	14	4.22	1.69	1.49	7.08	
	2.00	31	3.54	1.05	1.97	5.97	
OC-Vertical	3.00	40	4.29	0.94	2.13	6.87	**0.039**
	4.00	30	3.85	0.90	2.14	5.92	
	5.00	17	4.35	1.42	2.36	7.75	
	1.00	14	3.91	0.79	2.21	4.94	
	2.00	31	3.41	0.65	1.81	4.84	
OC-Horizontal	3.00	40	3.76	0.75	2.37	5.89	0.198
	4.00	30	3.74	0.88	2.19	6.64	
	5.00	17	3.89	1.07	2.47	6.56	
	1.00	14	13.40	6.8	2.99	26.90	
	2.00	31	10.56	4.4	2.90	24.78	
OC-Area (mm^2)	3.00	40	13.29	3.9	4.60	24.00	0.058
	4.00	30	12.90	5.5	3.00	33.00	
	5.00	17	14.84	5.8	6.36	24.80	
	1.00	14	95.74	29.2	59.70	157.00	
	2.00	31	77.88	30.4	25.27	167.00	
SOF-Area (mm^2)	3.00	40	92.82	28.8	34.75	157.00	0.229
	4.00	30	89.96	35.0	30.16	156.00	
	5.00	17	98.33	48.8	38.66	240.10	

Table V. Distribution of superior orbital fissure types according to sex.

Type	Female	Male	Total (%)	P value
1	10	9	19 (14.4)	
2	6	7	13 (9.8)	
3	9	7	16 (12.1)	
4	10	11	21 (15.9)	0.985
5	15	11	26 (19.7)	
6	10	7	17 (12.9)	
7	11	9	20 (15.2)	

highlighting the potential complications associated with surgical management. Their findings indicated that surgical manipulation of facial fractures may precipitate orbital apex syndrome, primarily due to elevated intraorbital pressure. Consequently, a comprehensive understanding of the normative anatomy and morphometric parameters of the orbital apex is indispensable for surgeons in accurately evaluating fracture extent and predicting associated clinical manifestations (Eo *et al*., 2005; Abed *et al*., 2011).

The occurrence of SOF syndrome also depends on the size of predisposing factors. An unexpectedly narrow SOF may result in compression of critical vessels and nerves passing through this region following trauma or surgery. Additionally, pressure from edema after injury or surgical intervention can further contribute to vascular and neural compression. In cases where the SOF is congenitally narrow, surgeons should exercise caution to avoid excessive manipulation of bony structures and compression of orbital tissues during fracture repair. A thorough understanding of anatomical variations is essential for accurately diagnosing the underlying causes of clinical conditions and for performing safe surgical procedures in this area (Kaur *et al*., 2022).

In a study conducted by Burdan *et al*. (2011), in Poles, the SOF area was found to be 93.713 mm^2 in females and 96.943 mm^2 in males. Furthermore, no statistically significant differences were observed between the sexes. Conversely, Mara and colleagues' findings, based on a 2016 study conducted with an Italian population, reported a median of 56.8±11.9 mm^2 in female subjects and 69.2±15.8 mm^2 in male subjects. Additionally, a statistical difference was observed between sexes (La Marra *et al*., 2016). In our study, the mean SOF area was 89.68±33.99 mm^2. The mean was 89.9±31.1 mm^2 in women and 89.5±36.5 mm^2 in men. There was no statistically significant difference between sexes. Our study showed similar results to those found in the study of Burdan *et al*. (2011).

OC morphometry and morphology are very important for clinicians and surgeons working in this field. The success of

Table VI. Comparison of measurements according to superior orbital fissure types.

Measurements	Type	N	Mean	S.D.	Min	Max	P
	1	19	19.05	1.87	17.22	23.46	
	2	13	19.88	2.02	17.29	23.60	
	3	16	16.57	4.15	8.826	22.69	
SOF-Length	4	21	22.81	2.72	18.07	28.41	**<0.001**
	5	26	20.54	2.70	16.08	25.11	
	6	17	20.24	2.40	13.28	23.27	
	7	20	13.94	3.73	8.55	21.43	
	1	19	2.06	0.87	0.73	4.16	
	2	13	2.48	0.93	1.36	5.20	
	3	16	2.29	0.94	0.79	4.05	
SOF-Width-Min	4	21	4.50	2.08	0.57	8.88	**<0.001**
	5	26	3.81	1.01	1.91	6.22	
	6	17	2.29	0.87	0.96	3.60	
	7	20	3.42	0.95	2.13	5.63	
	1	19	7.35	1.32	4.83	10.11	
	2	13	8.11	1.86	6.02	11.79	
	3	16	7.70	1.50	5.01	10.90	
SOF-Width-Max	4	21	8.70	1.71	5.54	12.41	**<0.001**
	5	26	8.76	1.60	6.54	12.44	
	6	17	5.44	1.25	3.03	7.84	
	7	20	7.26	1.75	4.03	10.02	
	1	19	15.59	2.21	11.62	19.51	
	2	13	16.15	2.10	13.13	19.32	
	3	16	13.12	4.27	5.77	19.90	
OC-Lateralpole-SOF	4	21	18.77	2.75	12.04	22.26	**<0.001**
	5	26	17.31	2.43	11.95	21.06	
	6	17	16.09	3.50	6.96	21.25	
	7	20	10.17	3.22	6.01	17.50	
	1	19	7.43	1.46	5.17	9.93	
	2	13	7.93	0.94	6.15	9.25	
	3	16	7.45	1.40	5.51	10.99	
OC-Medialpole-SOF	4	21	8.18	1.64	5.32	10.92	0.597
	5	26	7.70	1.12	5.57	9.53	
	6	17	7.88	2.12	5.47	13.08	
	7	20	7.40	1.53	4.920	11.10	
	1	19	7.83	1.15	5.82	9.56	
	2	13	8.82	1.74	6.35	12.44	
	3	16	8.55	1.24	6.19	10.42	
OC-Midpoint-SOF	4	21	9.34	1.98	6.23	13.65	**<0.001**
	5	26	9.35	1.62	6.81	13.78	
	6	17	7.40	1.34	5.34	9.64	
	7	20	7.96	1.98	5.28	12.88	
	1	19	4.043	1.20	2.13	5.97	
	2	13	4.00	1.49	1.97	7.75	
	3	16	3.72	1.00	2.03	5.94	
OC-Vertical	4	21	4.12	1.07	1.49	5.91	0.852
	5	26	4.18	1.14	2.05	6.87	
	6	17	3.76	1.12	1.91	5.98	
	7	20	4.11	1.20	2.52	7.08	
	1	19	3.57	0.80	2.37	5.89	
	2	13	3.53	0.81	2.01	4.51	
	3	16	3.80	1.17	1.81	6.56	
OC-Horizontal	4	21	3.82	0.82	2.19	5.14	0.798
	5	26	3.85	0.66	2.47	4.94	
	6	17	3.55	0.64	2.21	4.45	
	7	20	3.70	0.88	2.52	6.64	
	1	19	12.31	5.7	3.00	24.78	
	2	13	12.27	4.9	3.04	23.00	
	3	16	12.04	4.9	2.90	19.90	
OC-Area (mm^2)	4	21	13.84	4.3	4.60	21.10	0.652
	5	26	13.66	4.6	6.10	24.80	
	6	17	11.10	4.6	2.99	19.74	
	7	20	13.27	6.9	5.33	33.00	
	1	19	77.37	21.7	45.20	112.70	
	2	13	92.36	25.8	61.33	161.00	
	3	16	72.49	17.8	43.30	105.40	
SOF-Area (mm^2)	4	21	124.65	38.6	59.70	240.10	**<0.001**
	5	26	110.79	23.9	68.28	157.00	
	6	17	72.75	22.2	40.12	115.70	
	7	20	63.64	27.6	25.27	115.00	

interventions in conditions such as optic neuropathy, tumour or trauma depends on the knowledge of the important reference points of this area. The possibility of visual loss among the possible surgical complications indicates that the surgeon should work carefully and safely in this region (Zhang *et al*., 2013; Pirinc *et al*., 2023). In a study conducted by Jiang *et al*. (2015), in a Chinese population in 2015, the tranversal diameter of OC was 5.13 ± 0.38 mm (right side) and the vertical diameter was 5.97 ± 0.42 mm (right side). In a study conducted by Zhang *et al*. (2019), in the USA, with 335 individuals, the OC area was found to be 11.84±3.11 mm^2 . In another study, Bekerman *et al*. (2016) reported that the narrowest cross-sectional area of the normal OC was 13.85±2.89 mm^2. Bekerman *et al*. (2016) determined the OC area varied from 25.5 to 6.6 mm^2. In our study, the mean OC vertical diameter was 4.01±1.15 mm and the mean horizontal diameter was 3.71±0.82 mm. Furthermore, the mean OC area was recorded as 12.77±5.16 (2.90-33.00) mm^2. Our results are similar to the results in the literature. It is possible to assume that our lower and higher results are due to our more sensitive measurements.

In a study by Reymond *et al*. (2008), involving 100 cadavers, the morphometric relationships between the optic canal (OC) and superior orbital fissure (SOF) were evaluated. The study reported mean distances of 16.84 ± 2.95 mm (range: 9.2–24.6 mm) for OC to lateral pole of SOF, 10.88 ± 2.17 mm (range: 4.0–17.6 mm) for OC to medial pole of SOF, and 9.28 ± 1.51 mm (range: 4.1–16.0 mm) for OC to midpoint of SOF. In the present study, these measurements were found to be 15.43 ± 3.99 mm (range: 5.77–22.26 mm), 7.71 ± 1.49 mm (range: 4.92–13.08 mm), and 8.52 ± 1.75 mm (range: 5.28–13.78 mm), respectively. Our results closely correspond to those reported by Reymond *et al*. (2008) indicating consistency between the two studies.

Various classifications of SOF morphology have been proposed in the literature (Shapiro & Jansen, 1960; Reymond *et al*., 2008; Regoli & Bertelli, 2017; Pirinc *et al*., 2023; Erbek *et al*., 2024; Ercandırlı *et al*., 2025). In the study conducted by Shapiro & Janzen (1960) for the first time, SOF type was divided into 6 types. Reymond *et al*. (2008) divided the SOF type into 9 types and stated that there are two basic shapes

Table VII. Comparison of data according to Pearson correlation test.

	R and P value	Sex	SOF-Length	SOF-Width-Min	SOF-Width-Max	Type	OC-Lateralpole-SOF	OC-Medialpole-SOF	OC-Midpoint-SOF	OC-Vertical	OC-Horizontal	OC-Area (cm^2)	SOF-Area (cm^2)
Sex	r	1	0.014	-0.016	-0.051	-0.044	0.093	-0.107	0.060	-0.210	-0.018	-0.122	0.005
	p	1	0.870	0.857	0.562	0.615	0.287	0.221	0.496	0.016	0.838	0.163	0.952
SOF-Length	r		1	0.234	0.403	-0.205	0.912	0.174	0.366	0.266	0.222	0.341	0.709
	p		1	0.007	<0.001	0.019	<0.001	0.046	<0.001	0.002	0.011	<0.001	<0.001
SOF-Width-Min	r			1	0.548	**0.260**	0.191	0.277	0.509	0.166	0.195	0.243	0.622
	p			1	<0.001	0.003	0.028	0.001	<0.001	0.057	0.025	0.005	<0.001
SOF-Width-Max	r				1	-0.137	0.417	0.235	0.762	0.219	0.234	0.271	0.717
	p				1	0.117	<0.001	0.007	<0.001	0.012	0.007	0.002	<0.001
Type	r					1	-0.228	0.002	-0.042	0.015	0.042	0.035	-0.078
	p					1	0.009	0.982	0.629	0.862	0.633	0.686	0.376
OC-Lateralpole-SOF	r						1	-0.024	0.398	0.277	0.212	0.316	0.685
	p						1	0.784	<0.001	0.001	0.015	<0.001	<0.001
OC-Medialpole-SOF	r							1	0.378	-0.091	0.001	-0.074	0.269
	p							1	<0.001	0.301	0.993	0.402	0.002
OC-Midpoint-SOF	r								1	-0.003	0.124	0.104	0.652
	p								1	0.976	0.158	0.233	0.000
OC-Vertical	r									1	0.411	0.843	0.317
	p									1	<0.001	<0.001	<0.001
OC-Horizontal	r										1	0.693	0.295
	p										1	<0.001	0.001
OC-Area (mm^2)	r											1	**0.386**
	p											1	<0.001
SOF-Area (mm^2)	r												1
	p												1

in the form of egg or racket and the other shapes are the types that arise from the changes between these two basic shapes. Regoli & Bertelli (2017) stated that there is a diversity of different subtypes between these two shapes and it is very difficult to determine the subtypes. Moreover, in recent studies, Erbek *et al*. (2024) divided the SOF shape into 9 types, while Pirinc *et al*. (2023) and Erçandırlı *et al*. (2025) divided it into 7 types. In a study by Erçandırlı *et al*. (2025) using 3D CT images of 180 paediatric subjects, the least common type was narrow type with 7.2 % and the most common type was straight type with 20.8 %. In the study of Pirinc *et al*. (2023) the most common type was racket-shaped type (right: 24.5 % and left: 26 %) and the least common type was narrow type (right: 1 % and left: 2 %). Furthermore, no statistically significant difference was observed between sexes in terms of SOF types in both studies (p=0.150, p>0.05) (Pirinc *et al*., 2023; Erçandırlı *et al*., 2025). In our study, the most common type was Key-shaped type (19.7 %) and the least common type was Straight type (9.8 %). There was no statistically significant difference between the types in our study (p=0.985). In our study, measurements were also compared according to the types and no statistically significant difference was observed between the types only in the OC-Medialpole-SOF measurement. This indicates that all types have similar values in the distance of the SOF lower limit to the OC and may constitute a reference value.

This study has several limitations. It was conducted at a single center, which may limit the generalizability of the findings. Expanding the research to include multiple centers and a larger sample size would enhance the robustness and external validity of the results. Additionally, incorporating pediatric populations into the sample could provide valuable insights and further strengthen the study's impact.

In conclusion, this study comprehensively assesses the morphometry and morphology of the superior orbital fissure (SOF), the morphometry of the optic canal (OC), and the spatial morphometric relationship between these two critical anatomical structures. Given the vital neurovascular elements traversing the SOF and OC, as well as their close anatomical interplay, understanding their detailed morphometric characteristics is of paramount importance. Such knowledge holds significant clinical relevance, providing essential guidance for surgeons and clinicians in planning interventions and minimizing the risk of complications in this anatomically complex region.

ACKNOWLEDGMENTS. I would like to thank Mr. Ferhat Tunç, Architect, for providing technical support in the creation of the illustrations of the study.

ÖKSÜZLER, F.Y.; TUNÇ, M.; POLAT, S.; ÖZSAHIN, E.; ALTUN, Z. & GÖKER, P. Evaluación tridimensional de la morfometría y la relación espacial de la fisura orbitaria superior y el canal óptico. *Int. J. Morphol., 44(2)*:660-668, 2026-

RESUMEN: Este estudio tuvo como objetivo evaluar la morfología y la morfometría de la fisura orbitaria superior (FOS) y el canal óptico (CO), y analizar su relación espacial. Este estudio retrospectivo incluyó imágenes de tomografía computarizada dentomaxilofacial de 132 individuos sanos (71 mujeres y 61 hombres), con una edad media de 35,33 ± 11,48 años. Las imágenes se importaron a 3D Slicer (versión 5.6.2). Las mediciones del SOF incluyeron sus anchos mínimos y máximos, longitudes y áreas. Para el OC, se evaluaron los diámetros vertical y horizontal, así como el área. Adicionalmente, se registraron las distancias desde el OC a los puntos lateral, medio y medial del SOF. También se realizó la clasificación morfológica del SOF, categorizando su forma en siete tipos distintos. El análisis de subgrupos basado en la edad mostró diferencias significativas tanto en el diámetro vertical del canal óptico (p=0,039) como en el ancho mínimo de la fisura orbitaria superior (p=0,019) entre las diferentes décadas de edad. La clasificación morfológica del SOF identificó el tipo en forma de ojo de cerradura (Tipo 5) como la forma más prevalente (19,7 %), mientras que el tipo recto (Tipo 2) fue el menos frecuente (9,8 %). Se encontraron diferencias estadísticamente significativas en todos los parámetros morfométricos relacionados con el SOF entre los diferentes tipos morfológicos (p<0,05), excepto para la distancia entre el canal óptico y el margen lateral del SOF. El conocimiento exhaustivo de los parámetros morfométricos normativos es crucial no solo para una planificación quirúrgica precisa y una delimitación exacta de los límites operatorios, sino también para minimizar sustancialmente el riesgo de complicaciones intraoperatorias.

PALABRAS CLAVE: Fisura orbitaria superior; Ápice orbitario; Canal óptico; Morfometría; Morfología.

REFERENCES

Abed, S. F.; Shams, P.; Shen, S.; Adds, P. J. & Uddin, J. M. A cadaveric study of the morphometric and geometric relationships of the orbital apex. *Orbit., 30(2)*:72-6, 2011.

Bekerman, I.; Kimiagar, I.; Sigal, T. & Vaiman, M. Monitoring of Intracranial Pressure by CT-Defined Optic Nerve Sheath Diameter. *J. Neuroimaging, 26(3)*:309-14, 2016.

Burdan, F.; Umlawska, W.; Dworzanski, W.; Klepacz, R.; Szumilo, J.; Staros?awska, E. & Drop, A. Anatomical variances and dimensions of the superior orbital fissure and foramen ovale in adults. Folia Morphol. (Warsz.), 70(4):263-71, 2011.

Engin, O.; Adriaensen, G. F. J. P. M.; Hoefnagels, F. W. A. & Saeed, P. A systematic review of the surgical anatomy of the orbital apex. *Surg. Radiol. Anat., 43(2)*:169-78, 2021.

Eo, S.; Kim, J. Y. & Azari, K. Temporary orbital apex syndromeafter repair of orbital wall fracture. *Plast. Reconstr. Surg., 116(5)*:85e-89e, 2005.

Erbek, E.; Çiçekcibası, A. E.; Açar, G.; Digilli Ayas¸, B. & Aydog˘du, D. Morphometric evaluation of the anatomical relationships between the superior orbital fissure and the orbital structures based on computed tomography images with clinical implications. *Int. Ophthalmol., 44(1)*:267, 2024.

Erçandırlı, A. K.; Dolgun, H.; Alpergin, B. C.; Bozkurt, H.; Ülkü, G.; Kavcar, M.; Sezer, M. & Beger, O. Superior orbital fissure in children: shape analysis, measurements, and surgical importance. *Anat. Sci. Int., 100(2)*:198-206, 2025.

Jiang, P. F.; Dai, X. Y.; Lv, Y.; Liu, S. & Mu, X. Y. Imaging study on the optic canal using sixty four-slice spiral computed tomography. *Int. J. Clin. Exp. Med., 8(11)*:21247-51, 2015.

Kaur, A.; Delmotra, P.; Singh, K.; Kullar, J. S. & Sharma, R. K. Morphometric dimensions of superior orbital fissure: a cross-sectional study. *Int. J. Anat. Radiol. Surg., 11(3)*:AO26-8, 2022.

La Marra, A.; Quarchioni, S.; Ferrari, F.; Gravina, G. L.; Barile, A.; Gregori, L. M.; Di Cesare, E. & Splendiani, A. 640-Slice CT measurement of superior orbital fissure as gateway for light into the brain: statistical evaluation of area and distance. *PLoS One, 11(9)*:e0162940, 2016.

Li, L.; London, N. R. Jr.; Chen, X.; Prevedello, D. M. & Carrau, R. L. Expanded exposure and detailed anatomic analysis of the superior orbital fissure: Implications for endonasal and transorbital approaches. *Head Neck, 42(10)*:3089-97, 2020.

Pirinc, B.; Fazliogullari, Z.; Koplay, M.; Unver Dogan, N. & Karabulut, A. K. Morphometric and morphological evaluation of the optic canal in three different parts in MDCT images. *Int. Ophthalmol., 43(8)*:2703-20, 2023.

Radunovic, M.; Vukcevic, B.; Radojevic, N.; Vukcevic, N.; Popovic, N. & Vuksanovic-Bozaric, A. Morphometric characteristics of the optic canal and the optic nerve. *Folia Morphol. (Warsz.), 78(1)*:39-46, 2019.

Regoli, M. & Bertelli, E. The revised anatomy of the canals connecting the orbit with the cranial cavity. *Orbit, 36(2)*:110-7, 2017.

Reymond, J.; Kwiatkowski, J. & Wysocki, J. Clinical anatomy of the superior orbital fissure and the orbital apex. *J. Craniomaxillofac. Surg., 36(6)*:346-53, 2008.

Shapiro, R. & Janzen A. H. *The Normal Skull: A Roentgen Study*. Hoeber, New York, 1960.

Sinanoglu, A.; Orhan, K.; Kursun, S.; Inceoglu, B. & Oztas, B. Evaluation of optic canal and surrounding structures using cone beam computed tomography: considerations for maxillofacial surgery. *J. Craniofac. Surg., 27(5)*:1327-30, 2016.

Zhang, H.; Liu, X.; Cheng, Y.; Zhang, S.; Wang, C.; Cui, D.; Li, Y.; Fu, Y. & Wang, Y. A new method of locating the optic canal based on structures in sella region: computed tomography study. *J. Craniofac. Surg., 24(3)*:1011-5, 2013.

Zhang, X.; Lee, Y.; Olson, D. & Fleischman, D. Evaluation of optic canal anatomy and symmetry using CT. *BMJ Open Ophthalmol., 4(1)*:e000302, 2019.

Corresponding author:
Dr. Mahmut Tunç
Baskent University
Vocational School of Health Services
Department of Therapy and Rehabilitation
Adana
TURKEY

E-mail: fzt.mtunc@gmail.com

Orcid ID:0000-0003-1373-4700

	ORCID
Fatma Yasemin Öksüzler:	0000-0002-6886-9162
Sema Polat:	0000-0001-7330-4919
Esin Özsahin:	0000-0002-5261-4712
Zafer Altun:	0000-0002-6849-6458
Pınar Göker:	0000-0002-0015-3010